Journal of Inflammation Research

Dovepress
open access to scientific and medical research

Open Access Full Text Article

ORIGINAL RESEARCH

Preclinical Development of SHR-1819, a Potent Humanized IL-4Rα Antibody for Treating Type 2 Inflammatory Diseases

Guolin Zhao[1,2], Zhijun Wang[1,2], Jun Zhang[1,2], Yuan Lin[1,2], Tang Zhou[1,2], Kaili Liu[1,2], Changyong Yang[1], Cheng Liao[1]

[1]Department of Preclinical Research and Development, Jiangsu Hengrui Pharmaceuticals Co., Ltd., Lianyungang, Jiangsu, People's Republic of China; [2]Department of Preclinical Research and Development, Shanghai Shengdi Pharmaceutical Co., Ltd., Shanghai, People's Republic of China

Correspondence: Changyong Yang; Cheng Liao, Department of Preclinical Research and Development, Jiangsu Hengrui Pharmaceuticals Co., Ltd., Lianyungang, Jiangsu, 222000, People's Republic of China, Tel/Fax +86 021-61629291; +86 021-61063826, Email changyong.yang@hengrui.com; cheng.liao@hengrui.com

Background: Interleukin (IL)-4 and IL-13 are critical pathogenic factors for type 2 inflammation-related allergic diseases, sharing the mutual receptor subunit IL-4Rα. However, it was ineffective for certain type 2 inflammation diseases by targeting IL-4, IL-13 ligand alone or both in clinical studies. The work presented herein aimed to evaluate the preclinical efficacy and pharmacokinetics profile of a novel monoclonal antibody against IL-4Rα, SHR-1819, as a promising therapy for type 2 inflammation diseases.

Methods: SHR-1819 was generated through immunization by C57BL/6 mice with recombinant hIL-4Rα protein, followed by humanization and affinity maturation. Then, its binding properties with IL-4Rα were determined using surface plasmon resonance (SPR) and ELISA. In vitro inhibitory effects of SHR-1819 were assessed on hIL-4-/hIL-13-induced cell proliferation and signal transducer and activator of transcription 6 (STAT6) signaling activation. In vivo efficacy of SHR-1819 was evaluated in several type 2 inflammatory diseases models, including asthma, atopic dermatitis (AD), and allergic rhinitis (AR) by using hIL-4/hIL-4Rα transgenic mice. Furthermore, the pharmacokinetic (PK) profiles of SHR-1819 were characterized.

Results: SHR-1819 showed high binding affinity to human IL-4Rα and effectively blocked IL-4Rα at sub-nanomolar concentration. In vitro assays indicated that SHR-1819 significantly inhibited TF-1 cell proliferation and STAT6 activation induced by hIL-4/hIL-13. In the asthma model, SHR-1819 could reduce airway hyperresponsiveness, decrease serum IgE levels, and alleviated inflammatory lung cell infiltration. In the AD model, SHR-1819 could significantly alleviate inflammatory and skin symptoms. In the AR model, it could remarkably decrease the frequencies of nasal rubbing and sneezing, and inflammatory cell infiltration in nasal tissues. These in vivo efficacy studies demonstrated the therapeutic potential of SHR-1819 in preclinical disease models. Moreover, subcutaneous administration of SHR-1819 exhibited favorable bioavailability in mice.

Conclusion: The results supported SHR-1819 as a promising preclinical candidate for the treatment of type 2 inflammatory diseases, including asthma, AD and AR.

Keywords: type 2 inflammatory diseases, IL-4Rα, IL-4, IL-13

Introduction

The prevalence of allergic diseases has experienced a significant surge, reaching epidemic proportions and affecting more than one billion population worldwide.[1] Incidence of these diseases are higher in industrialized nations, as compared with developing countries. Meanwhile, incidence in developing countries is rising dramatically as urbanization and industrialization processing.[1] Studies have shown that allergic asthma and atopic dermatitis started to exhibit epidemic-level incidences since 1960s.[2–6] According to the latest studies, more than 50% of populations in Europe, Northern America, and Australia are suffering the allergen-specific IgE (to any allergen).[1]

Systemic hyperactivation of type 2 immune responses is commonly observed in various inflammatory disorders, including asthma, chronic rhinosinusitis (CRS) and atopic dermatitis (AD),[7,8] characterized by the presence of T helper 2

Received: 11 June 2024
Accepted: 7 September 2024
Published: 14 September 2024

(Th2) cells and type 2 innate lymphoid cells (ILCs), and upregulation of type 2 cytokines at the allergic sites. Escalated type 2 immunity and elevated IgE serum levels are common markers of AD, rhinosinusitis and asthma,[9] which may be the potential explanation for their co-occurrence in patients. Notably, both AD and asthma patients exhibit elevated levels of total and specific IgE, which could accelerate diseases progression upon exposed to aeroallergens.[10] Novel therapies targeting type 2 inflammation, such as biologics including anti-IgE (omalizumab), anti-IL-5 (mepolizumab, reslizumab), and anti-IL-5Rα (benralizumab), have been approved for asthma and may potentially be available for patients with chronic rhinosinusitis with nasal polyps in the future. Additionally, JAK1 inhibitors (upadacitinib, abrocitinib) have been approved for the treatment of atopic dermatitis (AD). However, there remains a lack of biologics for treating allergic rhinitis (AR).

IL-4 and IL-13 are two factors central to type 2 inflammation-related allergic diseases. IL-4 and IL-13 are structurally similar, and share the common receptor subunit IL-4Rα, both are playing critical roles in several biological events, such as chemokine production, impairment of the skin barrier, suppression of antimicrobial peptides, and allergic inflammation.[11] Both IL-4 and IL-13 are capable to induce Th2 cell differentiation, promote B cell class switching towards IgE production, and activate key hematopoietic/immune cells including mast cells, basophils, and macrophages. The intracellular signaling pathways mediated by IL-4Rα and the combination of IL-4/IL-13 are well-described as the Janus family protein kinases/signal transducer and activator of transcription (JAK/STAT) pathways.[12]

Given the crucial and overlapping roles of IL-4 and IL-13 in the pathogenesis of allergic diseases, targeting IL-4 and IL-13 might be a promising strategy for the treatment of allergic diseases. However, different targeting strategies may yield varying responses in clinical trials. For instance, focusing on IL-4 (eg, altrakincept, pascolizumab[13,14]) or IL-13 (eg, lebrikizumab, tralokinumab,[15–18] etc.) ligand individually, or even targeting both simultaneously (eg, pitrakinra[19]), may not yield adequate efficacy in asthma patients due to the complexity of asthma endotypes present in populations. Currently, there exists no pharmacological agent blocking IL-4 ligand in the treatment pipeline for AD, possibly because IL-13 is believed to play a preferential role in the effector phase of tissue type 2 inflammation.[20] So, the inhibition of IL-4 ligand is not regarded as a beneficial therapeutic strategy for type 2-mediated disorders. Conversely, targeting IL-4Rα seems to be the most effective approach for treating Th2 inflammation including asthma and AD.

In this study, we presented SHR-1819, a novel monoclonal antibody designed to bind human IL-4Rα (hIL-4Rα) and inhibit both IL-4 and IL-13 signaling. A series of in vitro and in vivo studies were performed to evaluate SHR-1819, and our findings demonstrated that SHR-1819 met the criteria as a clinical candidate potential for the treatment of IL-4/IL-13 related inflammatory diseases. Currently, SHR-1819 is undergoing clinical development as a potential therapy for asthma (NCT04772365) and severe atopic dermatitis (NCT06012812).

Methods

Antibody Generation and Affinity Determination

For the generation of the IL-4Rα antibody, C57BL/6 mice were immunized with recombinant human IL-4Rα protein. The splenocytes were isolated from the mice with the highest serum titer of antibodies against IL-4R and fused with myeloma cells (Sp2/0). The resulting hybridoma clones were screened for high affinity and antagonist activity. The total RNAs from the selected hybridoma were extracted and its cDNA was generated by RT-PCR. The DNA sequences of the variable regions of the heavy and light chains of the selected clones were obtained via DNA sequencing. Further humanization and affinity maturation were performed on the lead candidate, resulting in the final product, SHR-1819.

A surface plasmon resonance (SPR) assay was performed on a Biacore 8K system, to determine the binding kinetics for its interaction with IL-4Rα derived from human, cynomolgus monkey, rat, and mouse. Briefly, CM5 chip coated with human IL-4Rα was dipped into SHR-1819 at concentrations of 39 to 5000 nM with two-fold serial dilution. The process of molecular binding (180 seconds) and dissociation (300 seconds) was recorded using Biacore control software. The kinetics and affinity data were then analyzed with a 1:1 model using Biacore Insight Evaluation Software (V 2.0.15.12933).

Evaluation of IL-4Rα Binding Activity

The binding activity of SHR-1819 to human IL-4Rα (Sino Biological, Cat#10402-H08H) was determined by ELISA. A 96-well microtiter plate was directly coated with 1 μg/mL of IL-4Rα protein (50 μL per well), followed by subsequent addition of SHR-1819 and secondary antibody (HRP-conjugated anti-primary antibody) and HRP substrate TMB. The EC_{50} value of SHR-1819 binding to human IL-4Rα was then calculated.

Cellular Assays

TF-1 cells (ATCC CRL-2003) are lymphoma cells that express IL-4R and are sensitive to cytokines such as IL-4/IL-13. IL-4 could stimulate TF-1 cells to proliferate in the absence of granulocyte-macrophage colony-stimulating factor (GM-CSF). TF-1 cells were cultured in RPM11640 medium containing 10% FBS, 2 ng/mL GM-CSF (R&D, Cat#215-GM -010). 100 μL of cell suspension was added to a 96-well cell culture plate, at a density of 2×10^5 cells/mL. 50 μL of serially diluted antibodies to be tested and 50 μL of IL-4 (R&D, Cat#204-IL050) at a final concentration of 0.7 ng/mL were then added to each well. After incubation in an incubator (37°C, 5% CO_2) for 72 hours, the cell proliferation was detected using Cell-titer Glo kit (Promega, Cat#G7572) according to the manufacturer's instructions.

HEK-Blue IL-4 cells (Invivogen, Cat#hkb-stat6) were applied to test the effects of SHR-1819 on IL-4 signaling pathway. The cells were stably transfected with human IL-4R gene and STATE-mediated SEAP gene. The SEAP protein secreted into the supernatant can be detected by SEAP substrate QUANTI-Blue, which indicated the activation level of IL-4Rα signaling pathway. In brief, HEK-Blue IL-4 cells were cultivated in DMEM medium containing 10% FBS, 100 μg/mL Zeocin (Invivogen, Cat#ant-zn-05), and 10 μg/mL Blasticidin (Invivogen, Cat#ant-b1-05). 100 μL of cell suspension was added to a 96-well cell culture plate, at a density of 5×10^5 cells/mL. After culture for 24 hours (37°C, 5% CO_2), 100 μL of the serially diluted antibodies to be tested was added to each well. The culture plate was further incubated for 20–24 hours (37°C, 5% CO_2). Afterwards, 20 μL of cell supernatant was transferred from each well to a new 96-well flat bottom plate, 180 μL QUANTI–Blue substrate solution was added, and the culture plate was incubated in an incubator in dark for 1–3 hours. The absorbance at 620 nm was detected with a microplate reader for calculation of IC_{50}, as the criteria for inhibition on the IL-4 signaling pathway.

Animals

hIL-4/hIL-4Rα transgenic mice were purchased from Cyagen Biosciences and were used for in vivo studies. We have complied with all relevant ethical regulations for animal use from Institutional Animal Care and Use Committee (IACUC).

Ovalbumin (OVA)-Induced Asthma Model

All mice were randomly divided into different groups and were maintained in standard animal housing conditions (12 h light and 12 h dark cycles, and obtaining food and water *ad libitum*) of Animal Laboratory of Pharmalegacy. All protocols on mice were approved by the Animal Ethical and Welfare Committee of Pharmalegacy following the 8th edition of the *Guide for the Care and Use of Laboratory Animals*.

The mice were randomly divided into 4 groups (n=10/group): control, model and SHR-1819 (12.5 or 25 mg/kg) groups. On Days 1 and 14, all mice (except for the control group) were sensitized with intraperitoneal injections of 0.2 mg/mL of OVA solution (Sigma-Aldrich, St. Louis, MO, USA; grade V). On Days 28, 29, 30, 32, and 33, the animals were challenged with 1.5% OVA aerosol for 30 min daily. From Days 15 to 34, animals from each group were administered with the vehicle (5% glucose injection) or test articles via subcutaneous injection, at a frequency of once every 3 days.

Airway responsiveness was assessed on Day 31 using the Whole Body Plethysmograph system (Buxco BFL0100). All animals were aerosolized with 1.5625, 3.125, 6.25, 12.5, 25, 50 mg/mL methacholine (Mch), and each concentration was aerosolized for 90 seconds. Enhanced expiratory interval value (Penh) was measured at corresponding concentrations. The Penh value before aerosolized Mch administration was used as the baseline based on which the Penh change rate after inhalation of different concentrations of Mch was calculated.

On day 34, all mice were anesthetized with isoflurane and blood was collected. Then, animals were anesthetized by intraperitoneal injection of 25 mg/kg Sutai. Bronchoalveolar lavage fluid (BALF) was collected through instilling and retrieving 0.8 mL of phosphate buffer containing 1% bovine serum albumin (BSA) and 0.6 mM EDTA-K2 into the lung tissues, and the above process was repeated twice. Then, the BALF was centrifuged at 300 g for 5 min at 4°C, and the cell pellets were resuspended at a density of 10^7 cells/mL for counting eosinophils, neutrophils, lymphocytes and macrophages by Wright-Giemsa (BaSO, Zhuhai, Guangdong, China) staining. The total cell numbers in BALF were obtained by hemocytometer after trypan blue (Sigma-Aldrich, St. Louis, MO, USA) staining. Subsequently, mice were euthanized, and lung tissues were collected for histopathological examination.

The left lung lobes were fixed by 10% neutral-buffered formalin for 24 hours, and then embedded in paraffin. Paraffin-embedded sections (5 μm) were stained with haematoxylin/eosin (H&E) for histopathological examination. The slices were examined by a pathologist to obtain the histopathological parameters including airway diameter, mucosal thickness, and inflammatory cell infiltration scores (score 0–4, with 4 indicating the most severe injury).

Allergen-Induced AD Model

All mice were randomly divided into different groups and were maintained in standard animal housing conditions (12 h light and 12 h dark cycles, and obtaining food and water *ad libitum*) of Animal Laboratory of Shanghai Lab Animal Research Center.

The mice were randomly divided into 4 groups (n=10/group): control, model and SHR-1819 (12.5 or 25 mg/kg) groups. On Day 0, all animals (except for the normal control group) were sensitized by application of 1.5% oxazolone dissolved in acetone and olive oil. From Day 7 to day 34, the animals were challenged with 1% oxazolone on both ears (both sides) at a frequency of once every 72 hours. At the same time, the animals of each group were administered with the vehicle (5% glucose injection) or test articles via subcutaneous injection, once every 3 days. From day 0 to day 35, ear thickness was measured by a digital caliper. On day 35, blood was collected via the suborbital venous plexus for further serum IgE analysis. Subsequently, mice were euthanized and ear tissues were collected for histopathological examination.

The left ears were fixed by 10% neutral-buffered formalin for 24 hours, and then embedded in paraffin. Paraffin-embedded sections (5 μm) were stained with H&E Histological changes in the sections were graded on a scale of 0–3 based on the following criteria: inflammatory cell infiltration (0 = normal, 1 = mild, 2 = moderate, 3 = extensive); thickness of dermis (0: <40, 1: 40–60, 2: 60–80, 3: 1100 μm); and thickness of epidermis (0 = 1–2 layers, 1 = 2–3 layers, 2 = 3–4 layers, 3 = 4 layers or more).[21]

Allergen-Induced AR Model

All mice were randomly divided into different groups and were maintained in standard animal housing conditions (12 h light and 12 h dark cycles, and obtaining food and water *ad libitum*) of Animal Laboratory of Shanghai Xipur Bikai Experimental Animal Co., Ltd.

The mice were randomly divided into 5 groups (n=12/group): control, model and SHR-1819 (12.5, 25 or 50 mg/kg) groups. On Days 0, 7, and 14, all mice (except for the control group) were sensitized with intraperitoneal injections of 100 μg OVA/2 mg aluminum adjuvant. On Days 21 to 27, the animals were anesthetized with inhaled isoflurane (1.5–3%) and intranasally challenged with 500 μg of OVA. On Day 14 to 27, the animals of each group were administered with the vehicle (5% glucose injection) or test articles via subcutaneous injection at a frequency of once every 3 days.

On Day 27, symptoms of rhinitis within 10 minutes after the last challenge were recorded by video, and the frequencies of sneezing and rubbing per unit times were recorded. On Day 28, blood was collected via the suborbital venous plexus for further serum IgE analysis. Subsequently, mice were euthanized and nasal tissues were collected for histopathological examination.

Nasal tissues were embedded in 4% paraformaldehyde, sectioned, and stained with H&E. The slices were then examined by a light electron microscope. The intensity of inflammatory cell recruitment in nasal mucosa was graded using an arbitrary scale by the histopathologist.[22] All the slides were coded before analysis and read blindly to avoid observer bias.

Measurement of Serum IgE Concentrations

In the asthma, AD and AR models, serum was obtained by centrifuging the blood at 2000 g for 10 minutes, and IgE concentration was measured using the Mouse IgE Precoated ELISA kit (Dakewe) according to the manufacturer's instructions.

Pharmacokinetic Study

The hIL-4/hIL-4Rα transgenic mice were assigned into 2 groups. Each group contained 6 per sex for a total of 24 animals. Animals received a single administration of 50 mg/kg SHR-1819 via subcutaneous (SC) or intravenous (IV) injection, respectively. Then, whole blood was collected from animals at different time points before and after administration to prepare serum samples. A validated ELISA method was used to determine the serum concentrations of SHR-1819. Biotinylated IL-4R was used to capture SHR-1819 in 5% mouse serum, and Alexa Fluor TM 647 labeled Anti-Human IgG (Fc specific) was then added. The absorbance of laser excimer Alexa FluorTM 647 fluorescence (PMT 5%) was measured to calculate pharmacokinetic (PK) parameters using a non-compartmental model.

Statistical Analysis

Data were presented as mean ± SEM. Significant differences between groups were determined using Student's *t*-test or Dunnett's multiple comparisons test in GraphPad Prism version 9. $P < 0.05$ was considered statistically significant.

Results

SHR-1819 Showed High Affinity to Human IL-4Rα

The binding properties of SHR-1819 to IL-4Rα were determined by SPR and ELISA. The binding kinetic curves and parameters of SHR-1819 to human IL-4α were shown in Figure 1A and 1B, respectively. The results showed that SHR-1819 had robust binding affinity to human IL-4Rα, with K_D values of 1.32×10^{-10} M (Figure 1B). However, SHR-1819 exhibited no or very weak binding affinity to cynomolgus monkey, rat, or mouse IL-4Rα. Therefore, we used the transgenic mice expressed with human IL-4 and IL-4Rα for further in vivo evaluations. In the ELISA assay, SHR-1819 exhibited significant binding activity to human IL-4Rα, with an EC_{50} value of 0.116 nM (Figure 1C). Besides, the results showed that SHR-1819 effectively bound to B cells with EC_{50} values of 326.8 ng/mL in human samples (Figure 1D) and 7.225 ng/mL in hIL-4/hIL-4Rα transgenic mice (Figure 1E), respectively.

Finally, we evaluated the blocking ability of SHR-1819 to the hIL-4/hIL-4Rα interaction using an ELISA assay, with a result of IC_{50} value of 83.1 ng/mL (Figure 1F). These results demonstrated that SHR-1819 had a potent inhibitory effect on human IL-4Rα.

SHR-1819 Significantly Inhibited hIL-4- and hIL-13-Induced Cell Proliferation and STAT6 Activation

The binding of hIL-4 and hIL-13 to the Type I (IL-4Rα/γc) or Type II (IL-4Rα/IL-13Rα1) receptor complexes on TF-1 cells could trigger downstream signaling activation and subsequent cell proliferation. Thus, TF-1 cells were applied to assess the inhibitory effect of SHR-1819 on proliferation after stimulation by hIL-4 and hIL-13. The results indicated that SHR-1819 significantly inhibited hIL-4- and hIL-13-induced cell proliferation of TF-1 cells (Figure 2A and 2B), with IC_{50} values of 6.05 ng/mL and 16.59 ng/mL, respectively.

Moreover, binding of IL-4 or IL-13 to IL-4Rα could stimulate the phosphorylation of STAT6, which is a transcription factor to induce the expression of Th2-related cytokines. To investigate the impact of SHR-1819 on STAT6 signaling pathway, we used the HEK-Blue™ IL-4/IL-13 cells that stably expressing the reporter gene secreted embryonic alkaline phosphatase (SEAP), a downstream factor of STAT6. The activation of downstream STAT6 signaling by hIL-4 or hIL-13 could trigger the expression of SEAP in HEK293 cells, and thus the levels of SEAP in the supernatant reflected the effectiveness of SHR-1819. As Figure 2C and 2D showed, SHR-1819 significantly inhibited hIL-4- and hIL-13-induced STAT6 activation with IC_{50} values of 6.76 ng/mL and 3.78 ng/mL, respectively.

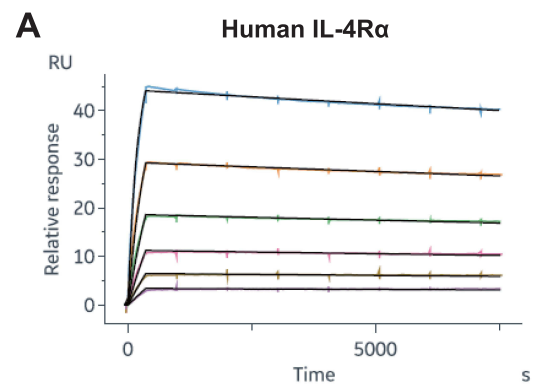

B Affinity of SHR-1819 to IL-4Rα from different species

Test ariticle	Species	K_a (1/Ms)	K_d (1/s)	K_D (M)
SHR-1819	Human	1.02E+05	1.34E-05	1.32E-10
	Cynomolgus	No or very weak binding		
	Rat	No or very weak binding		
	Mouse	No or very weak binding		

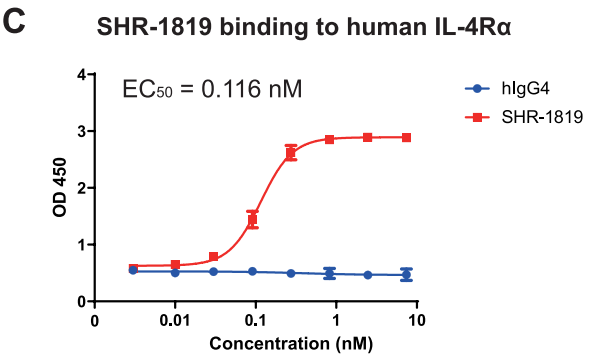

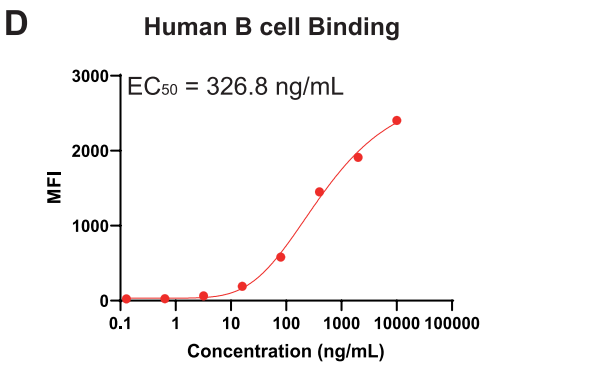

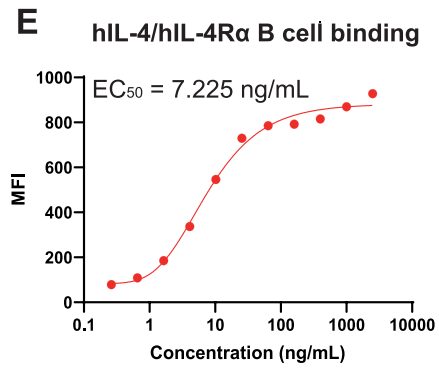

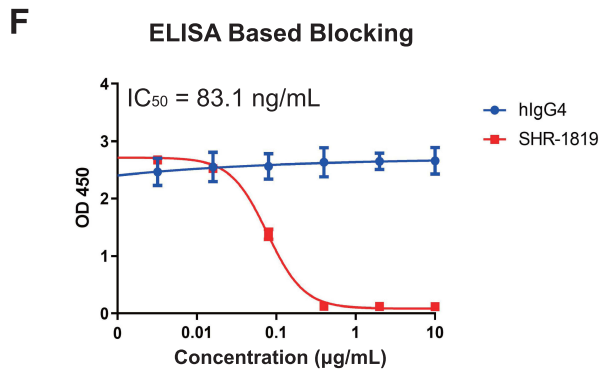

Figure 1 Binding and blocking profiles of SHR-1819. (**A**) and (**B**) Binding kinetics of SHR-1819 with human IL-4α by SPR. (**C**) Binding affinity of SHR-1819 to human IL-4Rα by ELISA. (**D**) and (**E**) Blocking profiles of SHR-1819 to IL-4Rα on B cells from human and hIL-4/hIL-4Rα transgenic mice by flow cytometry. (**F**) Blocking effect of SHR-1819 on hIL-4/hIL-4Rα by ELISA. Human IgG4 was used as a negative control.

SHR-1819 Showed Therapeutic Effects in the OVA-Induced Asthma Model

Asthma is a chronic condition characterized by airway inflammation, airway hyperresponsiveness (AHR), airflow obstruction, and airway wall remodeling.[23] Eosinophilic inflammation plays a crucial role in the pathogenesis of allergic asthma and is considered a prominent feature of asthmatic airways.[24] The OVA-induced asthma model in mice, characterized by eosinophilic asthma following OVA immunization, is a well-established model frequently used for evaluating potential therapeutic agents.[25,26] In this study, we established an OVA-induced asthma model in hIL-4/hIL-4Rα transgenic mice, and the protocol was shown in Figure 3A. From Day 15, the mice were subcutaneously administered with either vehicle or SHR-1819 (12.5 or 25 mg/kg) once every 3 days. No significant changes in body weight were observed during the whole study (Figure 3B), suggesting good tolerance for the SHR-1819 treatment.

To determine the effect on airway function, mice were exposed to increasing doses of methacholine aerosols. The model group showed increased airway hyperresponsiveness, as evidenced by an increase of Penh AUC (Figure 3C and 3D), while treatment of SHR-1819 (12.5 and 50 mg/kg) alleviated the airway hyperresponsiveness compared to

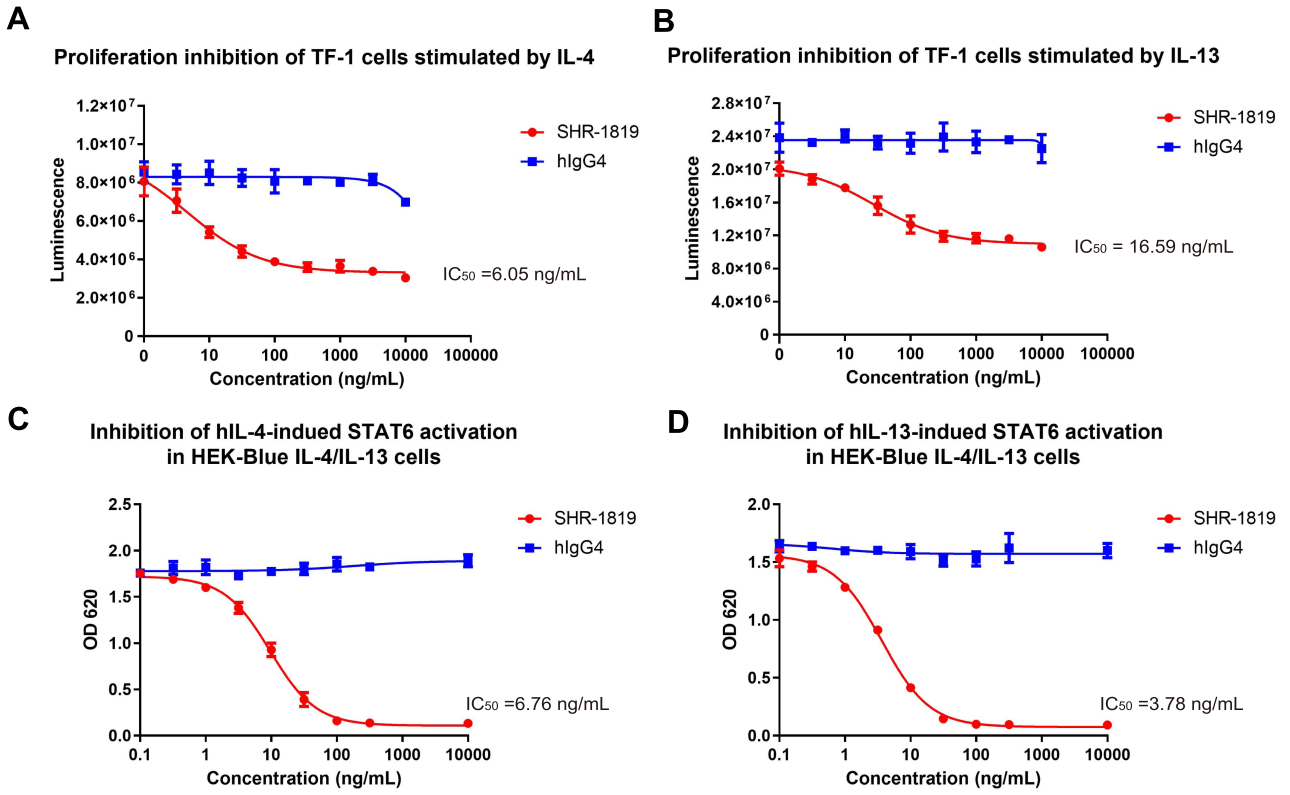

Figure 2 Cellular inhibitions of SHR-1819 on hIL-4 and hIL-13 signaling. (**A**) and (**B**) Inhibition on proliferation of TF-1 cells stimulated by IL-4 or IL-13. (**C**) and (**D**) Inhibition on STAT6 activation induced by hIL-4 or hIL-13 in HEK-Blue IL-4/IL-13 cells. Human IgG4 was used as a negative control.

the model group. On Day 34, SHR-1819-treated mice exhibited significantly reduced serum IgE levels, a marker of Th2 inflammation, as compared to the model group ($P < 0.001$, Figure 3E). Bronchoalveolar lavage fluid (BALF) was collected to investigate inflammatory cell recruitment. In comparison with the control group, the model group showed a substantial increase in the total number of cells, as well as increased numbers and percentages of eosinophils (Eso), macrophages (Mac), neutrophils (Neu) and lymphocytes (Lym) in BALF. After treatment of SHR-1819, a significant reduction ($P < 0.001$) in eosinophil and lymphocyte counts, and their percentages in BALF were observed (Figure 3F and 3G). Nevertheless, there was no notable effect on macrophages and neutrophils in BALF following SHR-1819 treatment.

Lung tissues were stained with hematoxylin and eosin (H&E) to evaluate inflammatory cell infiltration and mucus production. In Figure 3H, histological analysis of the model group showed the presence of numerous mucus plugs in the bronchial cavity, damaged airway epithelial cells, increased goblet cell proliferation, and substantial infiltration of inflammatory cells around the bronchi and blood vessels, as contrasted with the control group.[27] Treatment of SHR-1819 attenuated mucosal thickness, inflammation, and the overall lung score, with a noteworthy decrease observed in the high dose group (all $P < 0.05$, Figure 3I).

Collectively, administration of SHR-1819 significantly improved pathological markers in the OVA-induced asthma model using hIL-4/hIL-4Rα transgenic mice, suggesting SHR-1819 had the therapeutic potential for managing asthma.

SHR-1819 Exhibited Therapeutic Effects in the Oxazolone-Induced Atopic Dermatitis Model

AD is a chronic inflammatory skin disease characterized by symptoms such as rash, pruritus, eczema, xerosis and lichenification.[28] The oxazolone-induced mouse model is widely used to mimic AD-related symptoms. By repetitive

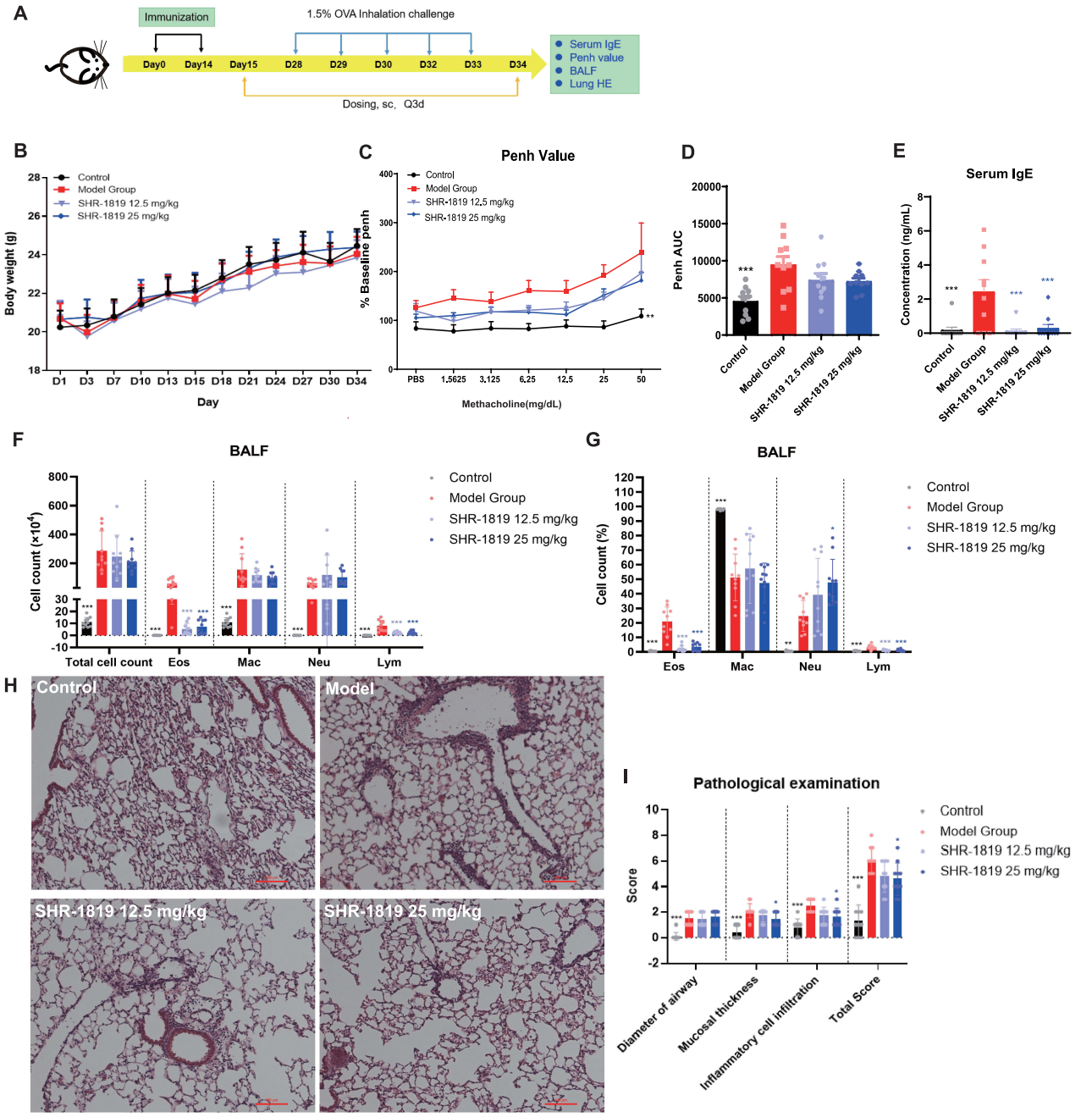

Figure 3 Effects of SHR-1819 on OVA-induced asthma in hIL-4/hIL-4Rα transgenic mice. (**A**) Protocol for the OVA-induced asthma model study in hIL-4/hIL-4Rα transgenic mice and administration of test articles. (**B**) Body weights during the treatment period. (**C**) The curve of Penh change rate against Mch concentration. (**D**) The area under the curve (AUC) of Penh curve on Day 31. (**E**) Serum IgE levels on Day 34, determined by ELISA. (**F**) and (**G**) Cell count and corresponding percentages of the Eos, Mac, Neu, and Lym cells in BALF, determined by FACS. (**H**) Representative H&E images of lung tissues. Bar =100 μm. (**I**) Scores of the histopathological parameters included airway diameter, mucosal thickness, and inflammatory cell infiltration (score 0–4, with 4 indicating the most severe injury). Data were presented as the sum of scores of each parameter. *P < 0.05, **P < 0.01, ***P < 0.001 vs Model Group using Student's t-test or Dunnett's multiple comparisons test in GraphPad Prism version 9.

exposure to oxazolone, a potent hapten, could induce a chronic Th2 hypersensitivity reaction similar to the initial stages of AD in humans.[28–30] In this study, we established an oxazolone-induced AD model in hIL-4/hIL-4Rα transgenic mice, with the experimental protocol shown in Figure 4A. From Day 7, the animals were subcutaneously injected with either vehicle or SHR-1819 once every 3 days.

As oxazolone-treated mice would exhibit AD-like skin symptoms, such as redness, swelling and increased ear thickness, we firstly evaluated the effects of SHR-1819 on ear thickness. The results showed that oxazolone treatment

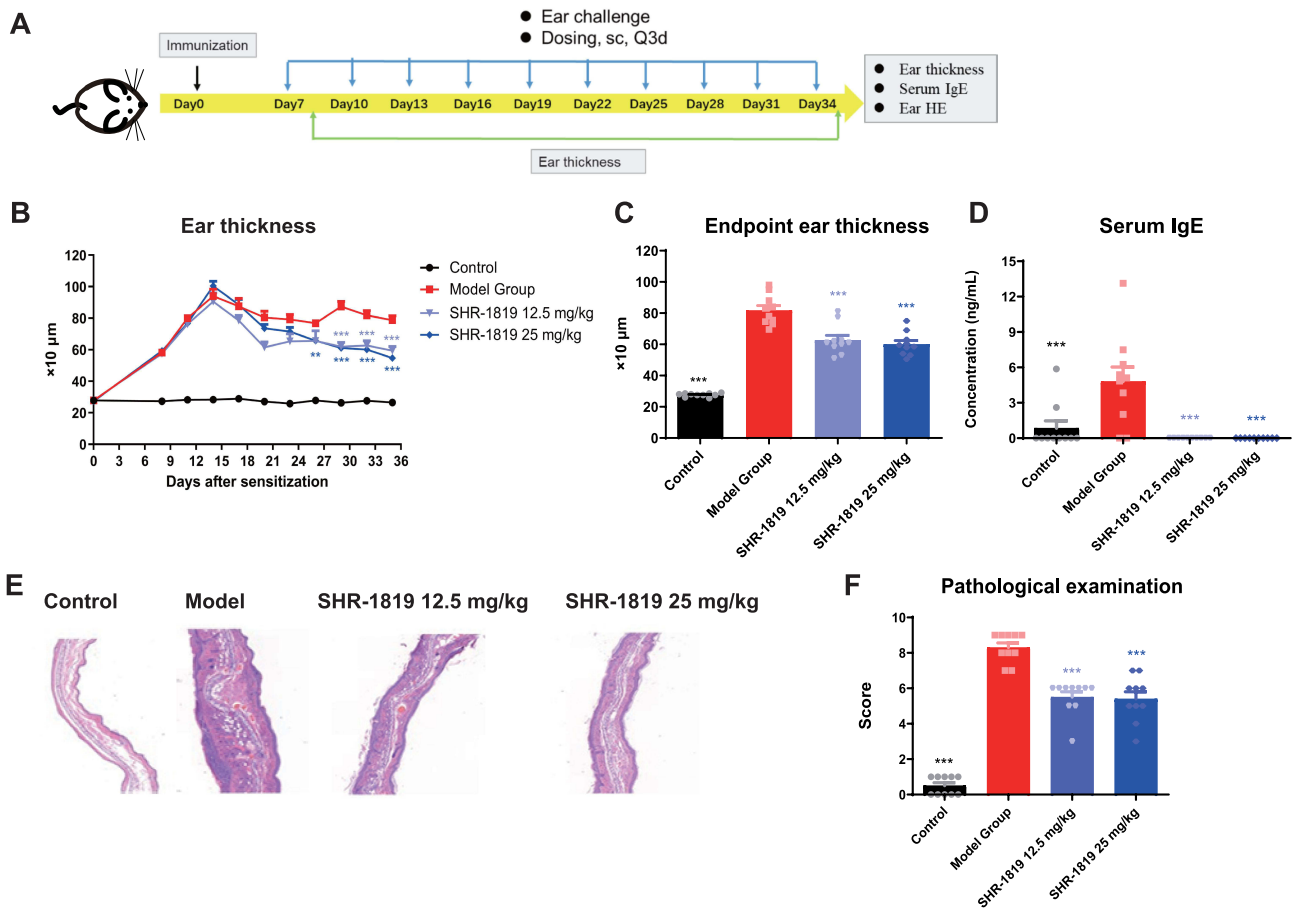

Figure 4 Effects of SHR-1819 on oxazolone-induced AD in hIL-4/hIL-4Rα transgenic mice. (**A**) Protocol for the oxazolone-induced AD model study in hIL-4/hIL-4Rα transgenic mice. (**B**) and (**C**) Ear swelling (thickness) was measured from Day 0 to Day 35. (**D**) Blood was collected and serum IgE levels were measured by ELISA. (**E**) Representative H&E images of ear tissues. (**F**) Scores of the histopathological parameters included inflammatory cell infiltration, dermal thickness, and epidermal thickness (score 0–3, with 3 indicating the most severe injury). Data were presented as the sum of scores of each parameter. $^{**}P < 0.01$, $^{***}P < 0.001$ vs Model Group using Student's *t*-test or Dunnett's multiple comparisons test in GraphPad Prism version 9.

caused a significant increase in ear thickness, as compared to that in the control group; while from D19, ear thickness in the SHR-1819 treatment groups were remarkably smaller than that in the model group (Figure 4B, $P < 0.001$). By the end of the experiment, the average ear thickness remained below 600 μm, which is statistically smaller than that in the model group ($P < 0.001$, Figure 4C). In the model group, serum IgE levels were significantly elevated after exposure to oxazolone, which could be reversed by SHR-1819 treatment (Figure 4D). To assess the benefits of SHR-1819 on histopathological features, the overall scores of epidermal thickness, dermal thickness, and inflammatory cell infiltration were further evaluated. Remarkably, SHR-1819 treatment resulted in a significant reduction in these parameters as compared to those of the model group (Figure 4E and 4F). These findings demonstrated that SHR-1819 could effectively alleviate inflammatory and atopic skin symptoms in the AD model.

SHR-1819 Demonstrated Therapeutic Effects in the OVA-Induced Allergic Rhinitis Model

AR is characterized by chronic inflammation of the nasal mucosa, accompanied by symptoms such as nasal itching, sneezing, and rhinorrhea. The OVA-induced AR mouse model has been commonly utilized to replicate the clinical symptoms of AR,[31] which is suitable to investigate the therapeutic effects of SHR-1819 on AR. After the last nasal OVA challenge on Day 27, the number of nasal rubbing and sneezing episodes within a 10-minute period was recorded for frequencies of nasal rubbing and sneezing (Figure 5A). Mice in the model group exhibited a significantly higher frequency of nasal rubbing and sneezing, compared to the control group (Figure 5B and 5C). Notably, SHR-1819

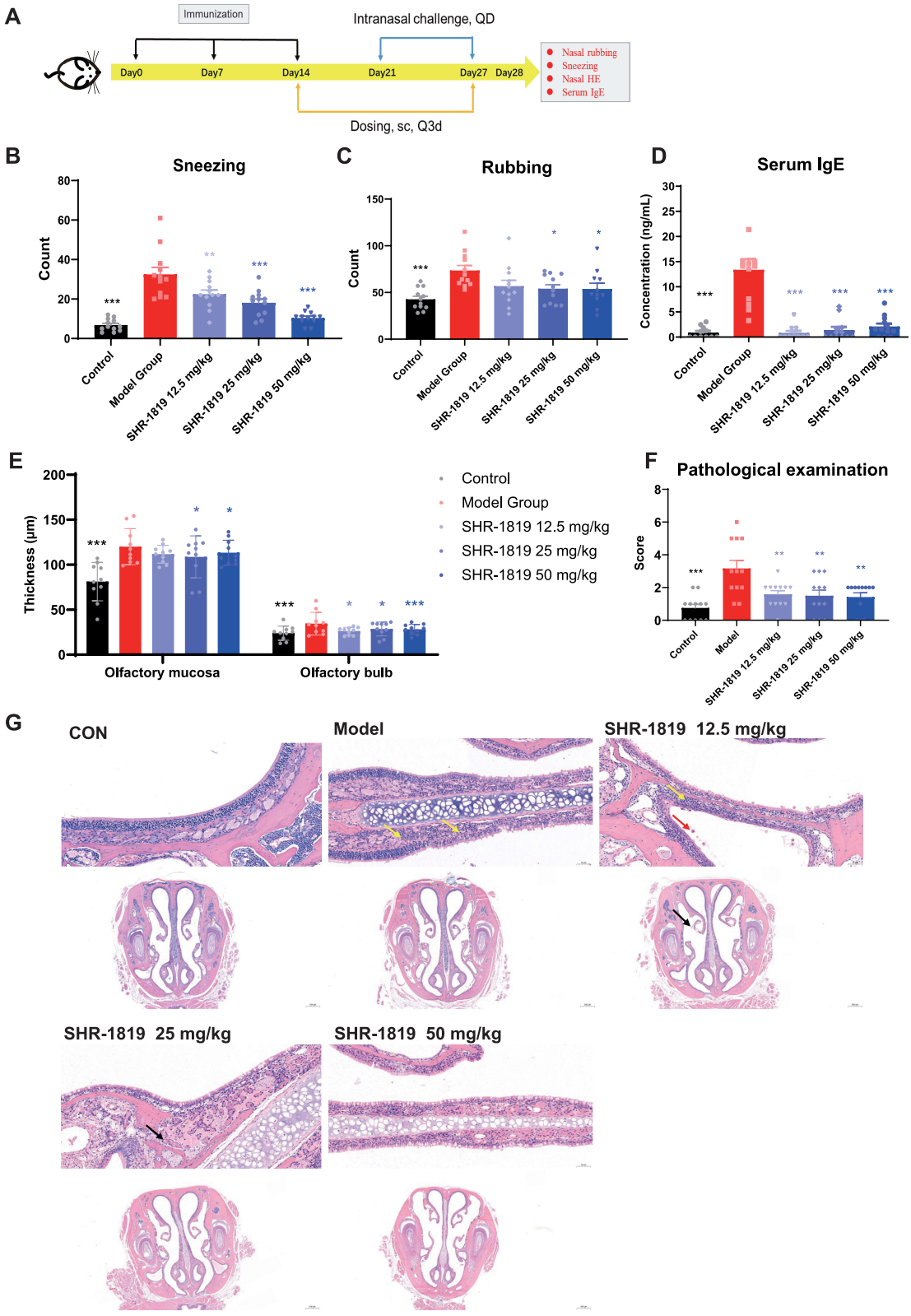

Figure 5 Effects of SHR-1819 on OVA-induced allergic rhinitis in hIL-4/hIL-4Rα transgenic mice. (**A**) Protocol for the OVA-induced allergic rhinitis mouse model study in hIL-4/hIL-4Rα transgenic mice. (**B**) and (**C**) Behavior changes (sneezing and rubbing counts) in OVA-induced model on Day 27. (**D**) Blood was collected and serum IgE levels were measured by ELISA. (**E**) and (**F**) Thickness of olfactory mucosa and olfactory bulb, and histopathological examination included morphology of mucosal epithelial cells and inflammatory cell infiltration (score 0–3, with 3 indicating the most severe injury). (**G**) Representative of H&E staining pictures of the mucous layer (upper image) and lamina propria (lower image). Yellow, black and red arrows indicated neutrophil and lymphocyte infiltration, epithelial shedding, and macrophage infiltration, respectively. Data were shown as the sum of scores of each parameter. *$P < 0.05$, **$P < 0.01$, ***$P < 0.001$ vs Model Group using Student's *t*-test or Dunnett's multiple comparisons test in GraphPad Prism version 9.

treatment resulted in a dose-dependent reduction in sneezing episodes in comparison with that in the model group ($P < 0.001$). In the SHR-1819-treated groups, nasal rubbing was also decreased, with significant changes observed in the middle and high dose groups ($P < 0.05$). Furthermore, there was a remarkable decrease in the levels of OVA-specific IgE in the SHR-1819-treated groups ($P < 0.001$) (Figure 5D).

As the nasal tissues are impaired under the AR condition, H&E staining was performed on sectioned nasal tissues to evaluate the thickness of the olfactory mucosa and olfactory bulb. Remarkably, SHR-1819 treatment resulted in a dose-dependent inhibition of olfactory mucosa and olfactory bulb thickness, with significant changes observed in the middle and high dose groups (Figure 5E). Additionally, following SHR-1819 treatment, there was a significant reduction in the histopathological score, which encompassed the morphology of mucosal epithelial cells and inflammatory cell infiltration (Figure 5F). Representative images of tissue slices were presented in Figure 5G. Notably, the histological features of the model group indicated noticeable neutrophil and lymphocyte infiltration in the mucous layer (yellow arrows). Although in the low dose SHR-1819 group, there was evidence of neutrophil and lymphocyte infiltration, as well as macrophage infiltration (red arrows) and epithelial shedding (black arrows), but these histological features were significantly attenuated in the middle and high dose groups. In conclusion, SHR-1819 effectively reduced AR symptoms and held the potential as a clinically efficient treatment for AR.

Pharmacokinetic Profile of SHR-1819 in hIL-4/hIL-4Rα Mice

The pharmacokinetic (PK) profile of SHR-1819 was evaluated in the hIL-4/hIL-4Rα transgenic mice. The results showed no notable differences in SHR-1819 concentrations following a single subcutaneous or intravenous injection of 50 mg/kg SHR-1819 (Figure 6). The elimination half-life ($t_{1/2}$) of subcutaneous administration was calculated as 67.5 hours. Additionally, the absolute bioavailability of subcutaneous administration was 84.7%. These PK data provided valuable insights for the translation of SHR-1819 into clinical settings.

Discussion

In recent years, emerging evidence highlighted the involvement of IL-4 and IL-13 in the pathogenesis of type 2 inflammatory diseases. Administration of IL-4 or IL-13 in mouse models has been shown to induce lung inflammation, characterized by increased infiltration of inflammatory cells particularly eosinophils, and upregulation of cytokines and chemokines in the lungs. These findings emphasized the critical role of IL-4 and IL-13 in the development of asthma and related phenotypes.[32] Various therapeutic strategies have been developed to target IL-4, IL-13, or IL-4Rα, including mutated ligands, soluble receptors, and antibodies.[33] Nevertheless, anti-IL-4Rα may be the most promising therapy in treating type 2 inflammatory diseases. In this study, we presented SHR-1819, a high affinity IgG4 monoclonal antibody that effectively blocked IL-4Rα with remarkable efficacies against mice models with asthma, atopic dermatitis, and allergic rhinitis, which demonstrated it as a promising therapy for type 2 inflammatory allergic diseases.

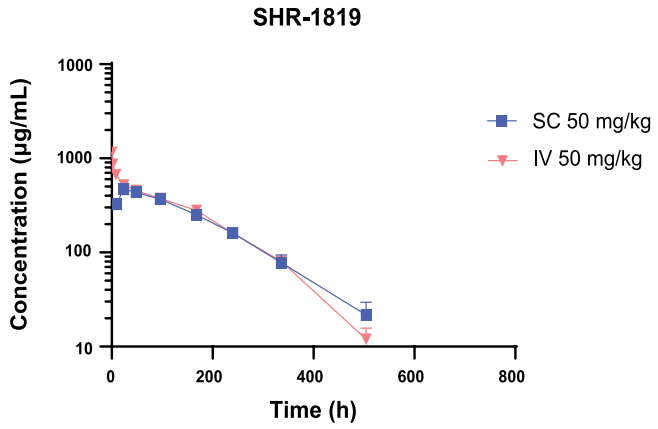

Figure 6 Mean concentration-time curves after a single subcutaneous (SC) or intravenous (IV) injection of SHR-1819 in hIL-4/hIL-4Rα transgenic mice.

IL-4 and IL-13 have been recognized for their distinctive roles in allergy and asthma pathogenesis.[34] IL-4 is involved in the regulation of T-cell proliferation, survival, and IgE synthesis,[11] while IL-13 plays a role in the late stages of the allergic reactions, such as airway remodeling and mucus hypersecretion.[11] In the present study, it is demonstrated that simultaneous blockade of both the IL-4 and IL-13 pathways could effectively reduce asthma-associated characteristics, such as inflammatory cell infiltration surrounding the bronchi and their associated vessels, as well as airway hyperresponsiveness.

IL-4 and IL-13 binding to IL-4Rα initiates the activation of tyrosine kinases 2 (Tyk2) and JAK1/2, subsequently leading to the activation of STAT transcription factors. The JAK-STAT pathway plays a critical role in the pathogenesis of AD.[12] Activation of the JAK-STAT pathway can negatively regulate the skin-barrier proteins and disrupt keratinocytes differentiation.[35,36] Furthermore, IL-4 signaling could promote Th2-cell activation. By activation of the JAK-STAT pathway, IL-4 signaling facilitates B-cell differentiation, resulting in the production of IgE by B-cells.[37–39] In vitro assays showed that SHR-1819 could significantly inhibit IL-4/IL-13-induced TF-1 cell proliferation and STAT6 activation, demonstrated the cellular potency and related mechanisms of SHR-1819.

In accordance with the "united airway disease hypothesis", asthma and allergic rhinitis are considered as the manifestations of the same inflammatory process mediated by Th2 cytokines like IL-4 and IL-13.[40] These two diseases commonly co-exist as comorbid conditions.[41] In our study, treatment with SHR-1819 could effectively alleviate allergic rhinitis symptoms, including decreased frequencies of sneezing and nasal rubbing, reduction of serum IgE levels, and diminished inflammatory cell infiltration of nasal tissues in a murine model. These findings collectively supported the evaluation of IL-4Rα-targeted therapy for patients with allergic rhinitis and asthma.

In a murine model of oxazolone-induced atopic dermatitis, treatment with SHR-1819 could attenuate atopic skin symptoms including ear swelling and decreased serum IgE levels, which were known to be induced by Th2 cytokines. Moreover, SHR-1819 also exhibited the capacity to modulate Th2 differentiation within the inflammatory infiltrate present in ear tissues, highlighting the potential of targeting IL-4Rα as a therapeutic approach for atopic dermatitis.

Furthermore, the subcutaneous administration of SHR-1819 obtained equivalent exposure as that through intravenous injection, and thus exhibited a relatively high bioavailability. The favorable pharmacokinetics profile enhanced its reliability and potential for successful translation into clinical practice.

In summary, our study has provided compelling evidence that SHR-1819, a high-affinity IL-4Rα antibody, held the immense promise as a therapeutic candidate for the treatment of Th2 inflammatory diseases, including asthma, AD and AR. Additionally, SHR-1819 has exhibited a favorable safety profile in healthy subjects during clinical evaluation (data not shown). Currently, Phase III trials have been initiated to evaluate the safety and efficacy of SHR-1819 in moderate to severe AD.

Conclusion

The current study demonstrated that SHR-1819, a novel IL-4Rα antibody, possessed high affinity and blocking activity of IL-4 and IL-13 signaling, and remarkable efficacies in murine models of asthma, atopic dermatitis, and allergic rhinitis. This research lays the groundwork for its translational potential in the treatment of Th2 inflammatory diseases. The long-term therapeutic potential and safety profile of SHR-1819 in the management of type 2 inflammatory diseases are currently being investigated through clinical practice.

Abbreviations

IL, interleukin; STAT6, signal transducer and activator of transcription 6; CRS, chronic rhinosinusitis; AD, atopic dermatitis; Th2, T helper 2; ILCs, innate lymphoid cells; JAK/STAT, Janus family protein kinases/signal transducer and activator of transcription; hIL-4Rα, human IL-4Rα; AR, allergic rhinitis; PK, pharmacokinetic; SPR, surface plasmon resonance; SEAP, secreted embryonic alkaline phosphatase; AHR, airway hyperresponsiveness; OVA, ovalbumin; BALF, bronchoalveolar lavage fluid; Eso, eosinophils; Mac, macrophages; Neu, neutrophils; Lym, lymphocytes; H&E, hematoxylin and eosin; $t_{1/2}$, elimination half-life; SC, subcutaneous; IV, intravenous; JAKs, Janus family protein kinase; Tyk2, tyrosine kinases 2.

Acknowledgments

The authors thank the colleagues that from the Department of Translational Medicine who participated in the studies. This work was funded by Jiangsu Hengrui Pharmaceuticals, Co., Ltd.

Disclosure

The authors declare no competing interest in this work.

References

1. Akdis CA. Does the epithelial barrier hypothesis explain the increase in allergy, autoimmunity and other chronic conditions? *Nat Rev Immunol*. 2021;21(11):739–751. doi:10.1038/s41577-021-00538-7
2. Platts-Mills TA. The allergy epidemics: 1870-2010. *J Allergy Clin Immunol*. 2015;136(1):3–13. doi:10.1016/j.jaci.2015.03.048
3. Eder W, Ege MJ, von Mutius E. The asthma epidemic. *N Engl J Med*. 2006;355(21):2226–2235. doi:10.1056/NEJMra054308
4. Bach JF. The effect of infections on susceptibility to autoimmune and allergic diseases. *N Engl J Med*. 2002;347(12):911–920. doi:10.1056/NEJMra020100
5. Backman H, Räisänen P, Hedman L, et al. Increased prevalence of allergic asthma from 1996 to 2006 and further to 2016-results from three population surveys. *Clin Exp Allergy*. 2017;47(11):1426–1435. doi:10.1111/cea.12963
6. Asher MI, Montefort S, Björkstén B, et al. Worldwide time trends in the prevalence of symptoms of asthma, allergic rhinoconjunctivitis, and eczema in childhood: ISAAC phases one and three repeat multicountry cross-sectional surveys. *Lancet*. 2006;368(9537):733–743. doi:10.1016/S0140-6736(06)69283-0
7. Zheng H, Zhang Y, Pan J, et al. The role of type 2 innate lymphoid cells in allergic diseases. *Front Immunol*. 2021;12:586078. doi:10.3389/fimmu.2021.586078
8. Hassoun D, Malard O, Barbarot S, Magnan A, Colas L. Type 2 immunity-driven diseases: towards a multidisciplinary approach. *Clin Exp Allergy*. 2021;51(12):1538–1552. doi:10.1111/cea.14029
9. Wise SK, Lin SY, Toskala E, et al. International consensus statement on allergy and rhinology: allergic rhinitis. *Int Forum Allergy Rhinol*. 2018;8(2):108–352. doi:10.1002/alr.22073
10. Ravnborg N, Ambikaibalan D, Agnihotri G, et al. Prevalence of asthma in patients with atopic dermatitis: a systematic review and meta-analysis. *J Am Acad Dermatol*. 2021;84(2):471–478. doi:10.1016/j.jaad.2020.02.055
11. Gour N, Wills-Karp M. IL-4 and IL-13 signaling in allergic airway disease. *Cytokine*. 2015;75(1):68–78. doi:10.1016/j.cyto.2015.05.014
12. Bao L, Zhang H, Chan LS. The involvement of the JAK-STAT signaling pathway in chronic inflammatory skin disease atopic dermatitis. *JAKSTAT*. 2013;2(3):e24137. doi:10.4161/jkst.24137
13. Akdis CA. Therapies for allergic inflammation: refining strategies to induce tolerance. *Nat Med*. 2012;18(5):736–749. doi:10.1038/nm.2754
14. Hart TK, Blackburn MN, Brigham-Burke M, et al. Preclinical efficacy and safety of pascolizumab (SB 240683): a humanized anti-interleukin-4 antibody with therapeutic potential in asthma. *Clin Exp Immunol*. 2002;130(1):93–100. doi:10.1046/j.1365-2249.2002.01973.x
15. Hanania NA, Korenblat P, Chapman KR, et al. Efficacy and safety of lebrikizumab in patients with uncontrolled asthma (LAVOLTA I and LAVOLTA II): replicate, Phase 3, randomised, double-blind, placebo-controlled trials. *Lancet Respir Med*. 2016;4(10):781–796. doi:10.1016/S2213-2600(16)30265-X
16. Panettieri RA, Sjöbring U, Péterffy A, et al. Tralokinumab for severe, uncontrolled asthma (STRATOS 1 and STRATOS 2): two randomised, double-blind, placebo-controlled, phase 3 clinical trials. *Lancet Respir Med*. 2018;6(7):511–525. doi:10.1016/S2213-2600(18)30184-X
17. Brightling CE, Chanez P, Leigh R, et al. Efficacy and safety of tralokinumab in patients with severe uncontrolled asthma: a randomised, double-blind, placebo-controlled, phase 2b trial. *Lancet Respir Med*. 2015;3(9):692–701. doi:10.1016/S2213-2600(15)00197-6
18. Gottlow M, Svensson DJ, Lipkovich I, et al. Application of structured statistical analyses to identify a biomarker predictive of enhanced tralokinumab efficacy in phase III clinical trials for severe, uncontrolled asthma. *BMC Pulm Med*. 2019;19(1):129. doi:10.1186/s12890-019-0889-4
19. Slager RE, Otulana BA, Hawkins GA, et al. IL-4 receptor polymorphisms predict reduction in asthma exacerbations during response to an anti-IL-4 receptor α antagonist. *J Allergy Clin Immunol*. 2012;130(2):516–22.e4. doi:10.1016/j.jaci.2012.03.030
20. Chiricozzi A, Maurelli M, Peris K, Girolomoni G. Targeting IL-4 for the treatment of atopic dermatitis. *Immunotargets Ther*. 2020;9:151–156. doi:10.2147/ITT.S260370
21. Watanabe N, Tomimori Y, Saito K, et al. Chymase inhibitor improves dermatitis in NC/Nga mice. *Int Arch Allergy Immunol*. 2002;128(3):229–234. doi:10.1159/000064256
22. Aswar U, Shintre S, Chepurwar S, Aswar M. Antiallergic effect of piperine on ovalbumin-induced allergic rhinitis in mice. *Pharm Biol*. 2015;53(9):1358–1366. doi:10.3109/13880209.2014.982299
23. Baarnes CB, Hansen AV, Ulrik CS. Enrolment in an asthma management program during pregnancy and adherence with inhaled corticosteroids: the 'management of asthma during pregnancy' program. *Respiration*. 2016;92(1):9–15. doi:10.1159/000447244
24. Uhm TG, Kim BS, Chung IY. Eosinophil development, regulation of eosinophil-specific genes, and role of eosinophils in the pathogenesis of asthma. *Allergy Asthma Immunol Res*. 2012;4(2):68–79. doi:10.4168/aair.2012.4.2.68
25. Lee MY, Seo CS, Lee NH, et al. Anti-asthmatic effect of schizandrin on OVA-induced airway inflammation in a murine asthma model. *Int Immunopharmacol*. 2010;10(11):1374–1379. doi:10.1016/j.intimp.2010.07.014
26. Yu QL, Chen Z. Establishment of different experimental asthma models in mice. *Exp Ther Med*. 2018;15(3):2492–2498. doi:10.3892/etm.2018.5721
27. Ou G, Liu Q, Yu C, et al. The protective effects of maresin 1 in the OVA-induced asthma mouse model. *Mediators Inflamm*. 2021;2021:4131420. doi:10.1155/2021/4131420
28. Jin H, He R, Oyoshi M, Geha RS. Animal models of atopic dermatitis. *J Invest Dermatol*. 2009;129(1):31–40. doi:10.1038/jid.2008.106

29. Zachariassen LF, Krych L, Engkilde K, et al. Sensitivity to oxazolone induced dermatitis is transferable with gut microbiota in mice. *Sci Rep*. 2017;7(1):44385. doi:10.1038/srep44385
30. Man MQ, Hatano Y, Lee SH, et al. Characterization of a hapten-induced, murine model with multiple features of atopic dermatitis: structural, immunologic, and biochemical changes following single versus multiple oxazolone challenges. *J Invest Dermatol*. 2008;128(1):79–86. doi:10.1038/sj.jid.5701011
31. Almansouri HM, Yamamoto S, Kulkarni AD, Ariizumi M, Adjei AA, Yamauchi K. Effect of dietary nucleosides and nucleotides on murine allergic rhinitis. *Am J Med Sci*. 1996;312(5):202–205. doi:10.1097/00000441-199611000-00002
32. May RD, Fung M. Strategies targeting the IL-4/IL-13 axes in disease. *Cytokine*. 2015;75(1):89–116. doi:10.1016/j.cyto.2015.05.018
33. Karo-Atar D, Bitton A, Benhar I, Munitz A. Therapeutic targeting of the interleukin-4/interleukin-13 signaling pathway: in allergy and beyond. *BioDrugs*. 2018;32(3):201–220. doi:10.1007/s40259-018-0280-7
34. Bitton A, Avlas S, Reichman H, et al. A key role for IL-13 signaling via the type 2 IL-4 receptor in experimental atopic dermatitis. *Sci Immunol*. 2020;5(44). doi:10.1126/sciimmunol.aaw2938
35. Esche C, de Benedetto A, Beck LA. Keratinocytes in atopic dermatitis: inflammatory signals. *Curr Allergy Asthma Rep*. 2004;4(4):276–284. doi:10.1007/s11882-004-0071-8
36. Bao L, Shi VY, Chan LS. IL-4 regulates chemokine CCL26 in keratinocytes through the Jak1, 2/Stat6 signal transduction pathway: implication for atopic dermatitis. *Mol Immunol*. 2012;50(1–2):91–97. doi:10.1016/j.molimm.2011.12.008
37. McKenzie AN, Culpepper JA, de Waal Malefyt R, et al. Interleukin 13, a T-cell-derived cytokine that regulates human monocyte and B-cell function. *Proc Natl Acad Sci*. 1993;90(8):3735–3739. doi:10.1073/pnas.90.8.3735
38. Yokota T, Otsuka T, Mosmann T, et al. Isolation and characterization of a human interleukin cDNA clone, homologous to mouse B-cell stimulatory factor 1, that expresses B-cell- and T-cell-stimulating activities. *Proc Natl Acad Sci*. 1986;83(16):5894–5898. doi:10.1073/pnas.83.16.5894
39. Pernis AB, Rothman PB. JAK-STAT signaling in asthma. *J Clin Invest*. 2002;109(10):1279–1283. doi:10.1172/JCI15786
40. Nur Husna SM, Md Shukri N, Mohd Ashari NS, Wong KK. IL-4/IL-13 axis as therapeutic targets in allergic rhinitis and asthma. *PeerJ*. 2022;10:e13444. doi:10.7717/peerj.13444
41. Hong H, Liao S, Chen F, Yang Q, Wang DY. Role of IL-25, IL-33, and TSLP in triggering united airway diseases toward type 2 inflammation. *Allergy*. 2020;75(11):2794–2804. doi:10.1111/all.14526